

Polymer Brushes on Periodically Nanopatterned Surfaces

Alexandros G. Koutsoubas[†] and Alexandros G. Vanakaras^{‡,*}

Department of Physics and Department of Materials Science, University of Patras, Patras 26504, Greece

Received August 5, 2008. Revised Manuscript Received September 24, 2008

Structural properties of polymer brushes tethered on a periodically nanopatterned substrate are investigated by computer simulations. The substrate consists of an alternating succession of two different types of equal-width parallel stripes, and the polymers are end-tethered selectively on every second stripe. Three distinct morphologies of the nanopatterned brush have been identified, and their range of stability has been determined in terms of a single universal parameter that combines the grafting density, the polymer length, and the stripe width. We propose scaling relations for the average brush height and for the architectural properties of the outer surface of the nanopatterned brush under good solvent conditions. Our analysis provides guidelines for fabricating well-defined and tunable nanopatterned polymeric films.

Introduction

Surface-initiated polymer brushes¹ have received considerable attention over the past years, mainly because they offer a promising way to modify, in a controllable fashion, a variety of physicochemical properties of surfaces.^{1–4} For a given linear polymer, statistically tethered on a specific substrate, the key parameters one can use to control the equilibrium properties of the system are the grafting density, the molecular weight, and the solvent quality. Theoretical studies^{5–10} on the equilibrium properties of such systems focus primarily on the mass distribution of the polymer above the substrate and/or the distribution of the free polymer ends. Predictions based on these considerations, usually in the form of general scaling relationships, are in qualitative agreement with experimental^{11–18} and computer simulation¹⁹ findings. They offer clear insight into how film morphology depends on experimentally controllable parameters

such as molecular weight, grafting density, solvent quality, and chemical affinity between polymer and substrate. The situation becomes rather complex when one moves from single-component linear flexible polymers to polymer mixtures or when the tethered macromolecules have higher architectural complexity, as in the cases of grafted copolymers,² dendrimers,^{20,21} or star-like polymers.² In these cases, the design parameters should include partial molecular weights in the case of grafted copolymers, the composition in the case of polymer mixtures, the generation in the case of dendrimers, or the number of arms in the case of star-like polymers.

Going beyond homogeneous polymer grafting to, for example, substrates subdivided into regions with distinct grafting properties, many interesting properties concerning the morphology of the polymeric layer are expected. Wenning et al. have shown²² that even local inhomogeneities of the grafting density may cause significant changes of the polymer distribution across the grafting surface. Recently, Patra et al., have studied by computer simulation^{23,24} and experiment²⁵ the structural properties of polymer brushes tethered selectively on well-defined regions of nanopatterned surfaces. Also, Daoulas et al. have investigated the self-assembly of a lamella-forming blend of a diblock copolymer on a periodically patterned substrate.²⁶ The results of the above works indicate that tethering polymers onto prepatterned substrates may lead to hybrid surfaces with novel morphologies that depend critically on the symmetry and the length scale of the substrate pattern.

The fabrication of nanopatterned polymer brushes relies, to a large extent, on the control of the substrate patterns. Recent advances in the nanostructuring of surfaces,²⁷ based mainly on nanolithographic and templating approaches, have provided such specific substrates, capable to tether selectively polymer

* Corresponding author. E-mail: a.g.vanakaras@upatras.gr.

[†] Department of Physics.

[‡] Department of Materials Science.

(1) Advincula, R. C.; Brittain, W. J.; Caster, K. C.; Rühle, J. *Polymer Brushes: Synthesis, Characterization, Applications*; Wiley: New York, 2004.

(2) Zhao, B.; Brittain, W. J. *Prog. Polym. Sci.* **2000**, *25*, 677.

(3) Brittain, W. J.; Minko, S. J. *Polym. Sci. A* **2007**, *45*, 3505.

(4) Zhou, F.; Huck, W. T. S. *Phys. Chem. Chem. Phys.* **2006**, *8*, 3815.

(5) Rühle, J.; Ballauff, M.; Biesalski, M.; Dziezok, P.; Grohn, F.; Johannsmann, D.; Houbenov, N.; Hugenberg, N.; Konradi, R.; Minko, S.; Motornov, M.; Netz, R. R.; Schmidt, M.; Seidel, C.; Stamm, M.; Stephan, T.; Usov, D.; Zhang, H. N. *Adv. Polym. Sci.* **2004**, *165*, 79.

(6) Alexander, S. J. *Phys. (Paris)* **1976**, *37*, 1443.

(7) de Gennes, P. G. *Macromolecules* **1980**, *13*, 1069.

(8) Milner, S. T.; Witten, T. A.; Gates, M. *Macromolecules* **1988**, *21*, 2610.

(9) Halperin, A.; Tirrell, M.; Lodge, T. P. *Adv. Polym. Sci.* **1991**, *100*, 31.

(10) Zhulina, E. B.; Borisov, O. V.; Brombacher, L. *Macromolecules* **1991**, *24*, 4679.

(11) Taunton, H. J.; Toprakcioglu, C.; Fetters, L. J.; Klein, J. *Nature* **1988**, *332*, 712.

(12) Auroy, P.; Auvray, L.; Leger, L. *Phys. Rev. Lett.* **1991**, *66*, 719.

(13) Auroy, P.; Mir, Y.; Auvray, L. *Phys. Rev. Lett.* **1992**, *69*, 93.

(14) Karim, A.; Satiya, S. K.; Douglas, J. F.; Anker, J. F.; Fetters, L. J. *Phys. Rev. Lett.* **1994**, *73*, 3407.

(15) Perahia, D.; Wiesler, D. G.; Satiya, S. K.; Fetters, L. J.; Sinha, S. K.; Milner, S. T. *Phys. Rev. Lett.* **1994**, *72*, 100.

(16) Field, J. B.; Toprakcioglu, C.; Ball, R. C.; Stanley, H. B.; Dai, L.; Barford, W.; Penfold, J.; Smith, G.; Hamilton, W. *Macromolecules* **1992**, *25*, 434.

(17) Kent, M. S.; Lee, L. T.; Farnoux, B.; Rondelez, F. *Macromolecules* **1992**, *25*, 6240.

(18) Baranowski, R.; Whitmore, M. P. *J. Chem. Phys.* **1995**, *103*, 2343.

(19) (a) Grest, G. S.; Murat, M. In *Monte Carlo and Molecular Dynamics Simulations in Polymer Science*; Binder, K., Ed.; Oxford University Press: New York, 1995; Chapter 9. (b) Daoulas, K. Ch.; Terzis, A. F.; Mavrantzas, V. G. *J. Chem. Phys.* **2002**, *116*, 11028. (c) Daoulas, K. Ch.; Mavrantzas, V. G.; Photinos, D. J. *J. Chem. Phys.* **2003**, *118*, 1521.

(20) Pickett, G. T. *Macromolecules* **2001**, *34*, 8784.

(21) Genson, K. L.; Holzmüller, J.; Villacencio, O. F.; McGrath, D. V.; Vaknin, D.; Tsukruk, V. V. *J. Phys. Chem. B* **2005**, *109*, 20393.

(22) Wenning, L.; Müller, M.; Binder, K. *Europhys. Lett.* **2005**, *71*, 639.

(23) Patra, M.; Linse, P. *Nano Lett.* **2006**, *6*, 133.

(24) Patra, M.; Linse, P. *Macromolecules* **2006**, *39*, 4540.

(25) Lee, W. K.; Patra, M.; Linse, P.; Zauscher, S. *Small* **2007**, *3*, 63.

(26) (a) Daoulas, K. C.; Müller, M.; Stoykovich, M. P.; Papakonstantopoulos, Y. J.; de Pablo, J. J.; Nealey, P. F.; Park, S.-M.; Solak, H. H. *J. Polym. Sci., Part B* **2006**, *44*, 2589. (b) Daoulas, K. C.; Müller, M.; Stoykovich, M. P.; Kang, H.; de Pablo, J. J.; Nealey, P. F. *Langmuir* **2008**, *24*, 1284.

(27) (a) Gates, B. D.; Xu, Q.; Stewart, M.; Ryan, D.; Willson, C. G.; Whitesides, G. M. *Chem. Rev.* **2005**, *105*, 1171. (b) Nie, Z.; Kumacheva, E. *Nat. Mater.* **2008**, *7*, 277.

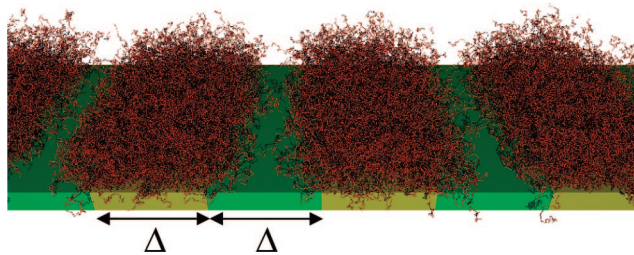


Figure 1. Representative snapshot of the studied system. The width of each grafting (yellow) and no grafting (green) stripe is Δ .

chains.^{28–35} In this context, the use of focused electron beams for the selective deactivation of polymerization initiators on a surface has led to fabrication of patterned polymer brushes with a lateral resolution of 50 nm.^{28–31} Very recently, new patterning methods^{33,34} such as nanografting, dip-pen nanolithography, contact lithography, and atomic force microscopy lithography³⁵ have produced surface motifs with resolution better than 10 nm. Taking into account that the height of a typical polymer brush lies in the range of a few up to several tens of nanometers, interesting and possibly exploitable nanoscale phenomena are expected when these two characteristic lengths are comparable.

In this work we study by means of Monte Carlo computer simulations the equilibrium morphology of systems composed of monodisperse linear homopolymers end-tethered on certain domains of a periodically patterned substrate. We study a specific class of grafting substrates that consist of two different types of equal-width parallel stripes with alternating capability, due to appropriate surface treatment, to tether the polymer chains. A representative snapshot of the studied system is given in Figure 1. The stripes are assumed infinitely long and their width, Δ , is the only parameter needed to describe this specific motif. We have examined in detail the equilibrium morphology of the patterned polymer brush as a function of the molecular weight (contour length), the surface coverage (grafting density) of the grafting stripes and the width of the stripes. The main body of our results concerns good solvent conditions although preliminary results of the same system under poor solvent conditions are also presented.

Brush Model and Computational Details

We have adopted the lattice bond fluctuation Monte Carlo (BFMC) method. The BFMC model for polymer chains has been originally proposed by Carmesin and Kremer³⁶ and has been applied successfully to the study of structure and dynamics of homogeneously end-grafted brushes.^{37–40} The BFMC method has the typical computational advantages of lattice MC methods

while the asymptotic limit of scaling laws related to chain behavior in the semidilute regime is achieved for relatively small chain contour lengths. On the other hand much longer chains are needed by off-lattice models^{41,42} to reproduce satisfactorily these scaling laws. We adopted the parametrization of references 37 and 38 according to which each monomer occupies eight lattice sites of a cubic lattice and the length of the allowed bond vectors connecting two neighboring monomers may be any of $2, \sqrt{5}, \sqrt{6}, 3$ or $\sqrt{10}$ lattice spacings. Hereafter all the lengths are measured in units of the lattice spacing. The grafted polymer ends are assumed rigidly attached to the surface, with each of them occupying an area of $s_0 = 2 \times 2$ since the closest distance of any pair of tethered ends is two lattice spacings. Similarly, nonbonded monomers are not allowed to approach closer than two lattice spacings. To take into account the quality of the solvent, we assume that each pair of nonbonded monomers contributes an amount ε to the internal energy of the system when their separation lies within $2 < r_{ij} \leq \sqrt{6}$. When $\varepsilon/k_B T < 0$ we implicitly impose poor solvent conditions while the athermal condition $\varepsilon/k_B T = 0$ corresponds to a very good solvent;³⁸ here k_B is the Boltzmann constant and T is the temperature.

The patterned substrate is modeled as a perfectly flat and impenetrable rectangular surface of size $L_x \times L_y$, on the xy plane at $z = 0$. It consists of $2m$ parallel domains (stripes) of equal width $\Delta (= L_x/2m)$, with the direction of the stripes defining the macroscopic y -axis. Polymer chains are allowed to tether at one end on every second stripe. The initial configuration of a system composed of K linear polymer chains of length N , is achieved by random end-grafting of K/m polymers on each grafting stripe. Since overlaps of the grafted ends are not allowed, the grafting density (surface coverage), σ_s , of the grafted stripes is $\sigma_s = s_0 K / (m \Delta L_y)$. Obviously, a system with grafting density at the grafting stripes, σ_s , has an overall surface coverage $\sigma = \sigma_s / 2$.

Results and Discussion

We have simulated more than 200 systems with polymer lengths in the range $30 \leq N \leq 100$, with surface coverage of the grafting stripes $\sigma_s = 0.05, 0.1, 0.2, 0.25$ and with stripe widths in the range $10 \leq \Delta < 500$. Simulations of nonpatterned uniformly grafted systems covering the above range of polymer lengths and grafting densities were performed as well. The main body of our simulation is devoted to systems under good solvent conditions ($\varepsilon/k_B T = 0$). In addition, we present preliminary results for systems under poor solvent conditions ($\varepsilon/k_B T < 0$). All the simulations are for $m = 3$ and $L_y = 100$ and with periodic boundary conditions in the x and y directions. In a single MC step, a monomer is chosen at random and a random displacement is attempted. On average, during a MC cycle we attempt one trial displacement on each monomer of the system. In each simulation the first 2×10^6 MC cycles are used for equilibration while ensemble averages are calculated in the course of the next $3–5 \times 10^6$ MC cycles. The length of these particularly long simulations is at least 10 times longer than the calculated chain relaxation time (in units of MC steps per monomer) in ref 37. Furthermore, several averages, including brush height and its variance, were monitored during the simulation runs to serve as a direct check of equilibration. All these indicators were consistent with well-equilibrated systems.

The monomer average density profile, $\phi(z; \Delta, N, \sigma_s)$, above the grafting surface is a directly measurable distribution through neutron reflectivity measurements.^{14–16} It contains important information about the equilibrium properties of the brush, and

(28) Brack, H.-P.; Padeste, C.; Slaski, M.; Alkan, S.; Solak, H. H. *J. Am. Chem. Soc.* **2004**, *126*, 1004.

(29) Padeste, C.; Solak, H. H.; Brack, H.-P.; Slaski, M.; Gursel, S. A.; Scherer, G. G. *J. Vac. Sci. Technol. B* **2004**, *22*, 3191.

(30) Schmelmer, U.; Jordan, R.; Geyer, W.; Eck, W.; Golzhauser, A.; Grunze, M.; Ulman, A. *Angew. Chem.* **2003**, *42*, 559.

(31) Maeng, L. S.; Park, J. W. *Langmuir* **2003**, *19*, 9973.

(32) Konradi, R.; Ruhe, J. *Langmuir* **2006**, *22*, 8571.

(33) Christman, K. L.; Enriquez-Rios, V. D.; Maynard, H. D. *Soft Matter* **2006**, *2*, 928.

(34) Jhaveri, S. B.; Beinhoff, M.; Hawker, C. J.; Carter, K. R.; Sogah, D. Y. *ACS Nano* **2008**, *2*, 719.

(35) Martinez, R. V.; Losilla, N. S.; Martinez, J.; Huttel, Y.; Garcia, R. *Nano Lett.* **2007**, *7*, 1846.

(36) Carmesin, I.; Kremer, K. *Macromolecules* **1988**, *21*, 2819.

(37) Lai, P.-Y.; Binder, K. *J. Chem. Phys.* **1991**, *95*, 9258.

(38) Lai, P.-Y.; Binder, K. *J. Chem. Phys.* **1992**, *97*, 586.

(39) Deutsch, H. P.; Binder, K. *J. Chem. Phys.* **1991**, *94*, 2294.

(40) Wittmer, J.; Joanny, J. F.; Binder, K. *J. Chem. Phys.* **1994**, *101*, 4379.

(41) Grest, G. S.; Murat, M. *Macromolecules* **1993**, *26*, 3108.

(42) Grest, G. S. *Macromolecules* **1994**, *27*, 418.

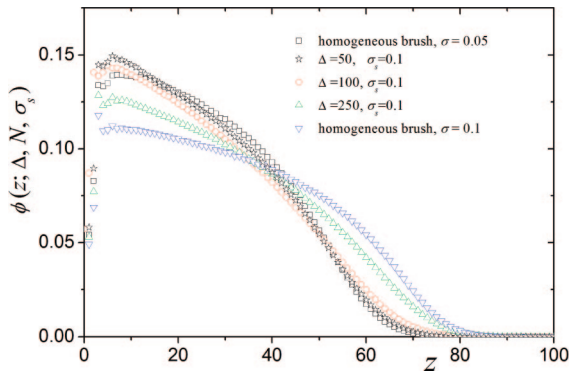


Figure 2. Monomer density profile ϕ , for systems with $N = 60$ and $\sigma_s = 0.1$, for various pattern widths, Δ . The two limiting cases corresponding to homogeneous brushes with grafting densities σ_s and $\sigma_s/2$ are also plotted.

its direct experimental realization serves as a critical test for both theory and simulations of brushes. We calculate this profile as $\phi(z; \Delta, N, \sigma_s) \equiv 1/A \langle \sum_{i=1}^K \sum_{n=0}^N \delta(z - z_{i;n}) \rangle$; here, $z_{i;n}$ is the projection of the position vector of the i th monomer of the n th polymer chain on the z -axis, A is the surface area, and the brackets denote ensemble average. For a uniformly grafted brush in a good solvent, both theory and simulations predict that the density profile, $\phi_u(z; N, \sigma)$ shows a typical parabolic dependence on z and a long decaying tail at the end of the distribution.

In Figure 2 we present calculated density profiles $\phi(z; \Delta, N, \sigma_s)$ for systems with $N = 60$ and $\sigma_s = 0.1$ on substrates of various stripe widths. For comparison, we also plotted in the same graph the density profiles $\phi_u(z; N, \sigma)$ of nonpatterned brushes with $N = 60$ and grafting densities $\sigma = 0.1$ and $\sigma = 0.05$. We note here that the short ranged density oscillation very close to the grafting substrate is due to the nature of the bond fluctuation model, as explained in detail in ref 37. From this plot, some first conclusions can be drawn: (i) When $\Delta/N < 1$, i.e., chains with contour length shorter than the stripe width, the patterned brush exhibits a density profile that is very similar to the corresponding profile of a homogeneously grafted brush with grafting density σ ($= \sigma_s/2$). This similarity suggests that the space above the uncovered stripes is well populated with monomers and the effect of the patterned surface is practically lost even at very short distances from the substrate. However, a closer examination of the tail of the distributions in this regime ($\Delta/N < 1$) reveals that the patterned brush appears slightly more elongated than the corresponding homogeneous brush with grafting density σ . This finding suggests that, although both brushes have the same overall grafting density, σ , the patterned brush appears slightly more extended as a result of the locally higher grafting densities imposed by the patterned surface. (ii) When $\Delta/N \gg 1$, the brushes on the grafted stripes become independent, and the density profile of the patterned systems tends to become similar to the corresponding profile of a homogeneous brush with grafting density equal to σ_s . However, in accordance to the findings of Patra et al., the bulk behavior is not recovered, even when $\Delta \approx 10N$ as a result of the lateral swelling of the individual brushes. (iii) In the intermediate regime, when Δ is comparable or slightly greater than N , the density profile is intermediate between the two limiting cases and exhibits nontrivial behavior. In this regime, the morphology of the overall brush is determined by the interplay between the entropic tendency to swell laterally, in order to cover the empty space of the adjacent nongrafted stripes and the steric interactions among the successive sub-brushes that prevent extended lateral swelling. Similar

behavior is observed for all the studied systems, irrespective of their grafting densities and polymer lengths.

The first moment of $\phi(z; \Delta, N, \sigma_s)$ gives the equilibrium mean brush height: $\bar{z}(\Delta, N, \sigma_s) = [\int dz z \phi(z; \Delta, N, \sigma_s)] / [\int dz \phi(z; \Delta, N, \sigma_s)]$. Both self-consistent field (SCF) theories⁸ and computer simulations of uniformly grafted polymer brushes under good solvent conditions^{37,40} predict, in accordance with scaling arguments,^{6,7} that the average brush height, $\bar{z}_u(N, \sigma)$ obeys the scaling law $\bar{z}_u(N, \sigma) \propto N\sigma^{1/3}$. This relationship, strictly valid for semidilute brushes, is confirmed by our simulations for all the systems with $N\sigma^{1/3} > 13$. The systems with $\sigma = 0.05$, $N = 60$ and with $\sigma = 0.1$, $N = 30$ deviate slightly from this scaling law since, according to Wittmer et al.,⁴⁰ they fall in the boundary between the mushroom and the semidilute regime. We use the ratio $q(\Delta, N, \sigma_s) = \bar{z}(\Delta, N, \sigma_s) / \bar{z}_u(N, \sigma_s/2)$ as a direct measure of the deviation of the patterned brush height from the corresponding mean height of a homogeneously grafted system with the same overall grafting density. According to the previous qualitative analysis of the density profiles, we expect that, for $\Delta/N \ll 1$, $q(\Delta \ll N, \sigma_s) \approx 1$, and for $\Delta/N \gg 1$, $q(\Delta \gg N, \sigma_s) \approx 2^{1/3}$. Indeed, as we can see from Figure 3a, where we plot $q(\Delta, N, \sigma_s)$ as a function of Δ/N , this is the case for $\Delta/N \ll 1$. The other limiting case, $\Delta/N \gg 1$, requires simulations of very large systems; however, the behavior of the plotted curves suggests that this limit is approached, at least for the systems with the higher grafting density, when $\Delta/N > 20$. From the same plot it appears that the critical value of Δ/N , at which the patterned brush departs from the homogeneous brush behavior, depends on the grafting density at the grafting stripes. A closer examination of Figure 3a reveals that this departure occurs at lower Δ/N upon decreasing the grafting density. In Figure 3b we plot $q(\Delta, N, \sigma_s)$ as a function of $\xi \equiv \Delta / (N\sigma_s^{1/3})$. With this rescaling, the data points collapse fairly accurately, at least up to $\xi \approx 10$, to a single curve. This implies that the dependence of the average brush height $\bar{z}(\Delta, N, \sigma_s)$ factors as

$$\bar{z}(\Delta, N, \sigma_s) = \bar{z}_u(N, \sigma_s/2) q(\xi) \quad (1)$$

where $q(\xi)$ is a universal function of $\xi = \Delta / (N\sigma_s^{1/3})$. We suggest the following functional form for $q(\xi)$:

$$q(\xi) = \begin{cases} 1 & \xi \leq \xi_0 \\ 2^{1/3} - (2^{1/3} - 1)e^{-a(\xi - \xi_0)} & \xi > \xi_0 \end{cases} \quad (2)$$

This equation satisfies both limiting conditions since for $\xi < \xi_0$, $q(\xi) = 1$, and for $\xi \gg \xi_0$ we have $q(\xi) = 2^{1/3}$. Choosing $a = 0.12$ and $\xi_0 = 2.5$, we get a satisfactory fit (the thick solid line in the plot of Figure 3b) of the calculated data for the whole range of ξ .

In order to examine in more detail the morphology of the patterned brush we calculated the two-dimensional density profile $\phi(x, z; \Delta, N, \sigma_s) \equiv (1/L_y) [\langle \sum_{i=1}^K \sum_{n=0}^N \delta(z - z_{i;n}) \delta(x - x_{i;n}) \rangle]$, which gives the equilibrium probability density to find a monomer at x, z , irrespective of its y -coordinate. The corresponding density profile of the free ends of the chains, $\phi_e(x, z; \Delta, N, \sigma_s) \equiv (1/NL_y) [\langle \sum_{i=1}^K \delta(z - z_{i;n}) \delta(x - x_{i;n}) \rangle]$, gives important information for the distribution of the free ends of the polymer above the grafting surface, but it is inefficient to provide a clear picture of the outer surface of the brush due to extensive backfolding of the free ends of the chains. To quantify the morphology of the outer surface of the grafted polymer, we define the perimeter of the brush as the thin layer that is characterized by a monomer volume fraction $\phi(x, z)$ within the range $\phi_0 \pm 0.005$. Solving the inequality $|\phi(x, z) - \phi_0| \leq 0.005$ at x , we obtain a range of z 's located within a small interval centered at $h_{\phi_0}(x)$. This function gives the ϕ_0 "level" of the perimeter of the brush as a function of x .

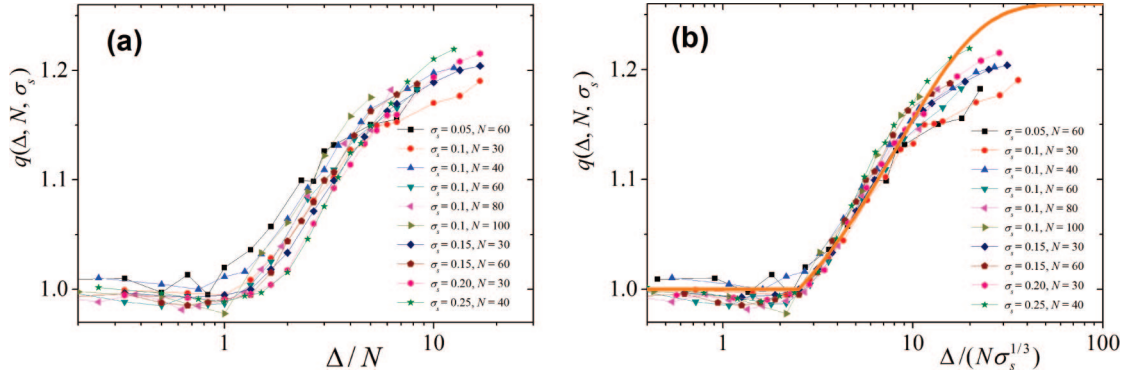


Figure 3. Plots of the ratio $q(\Delta, N, \sigma_s) = \bar{z}(\Delta, N, \sigma_s) / \bar{z}_0(N, \sigma_s/2)$ as a function of (a) Δ/N and (b) $\xi = \Delta/(N\sigma_s^{1/3})$. The solid line in (b) has been obtained using eq 2 with parameters $a = 0.12$ and $\xi_0 = 2.5$.

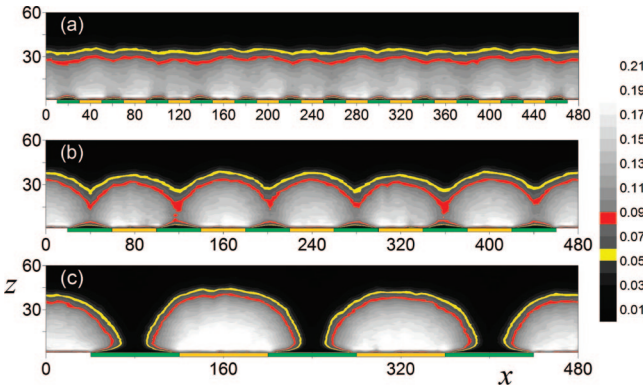


Figure 4. Representative contour plots of the average two-dimensional density profile $\phi(x, z)$ for the system with $N = 40$ and $\sigma_s = 0.1$ for various stripe widths: (a) $\Delta = 20$ ($\xi = 1.08$), (b) $\Delta = 40$ ($\xi = 2.15$), and (c) $\Delta = 80$ ($\xi = 4.31$). The yellow and red contours correspond to $\phi_0 = 0.05$ and 0.08 , respectively. The alternating green and orange bars on the x -axis represent the grafting and nongrafting stripes, respectively.

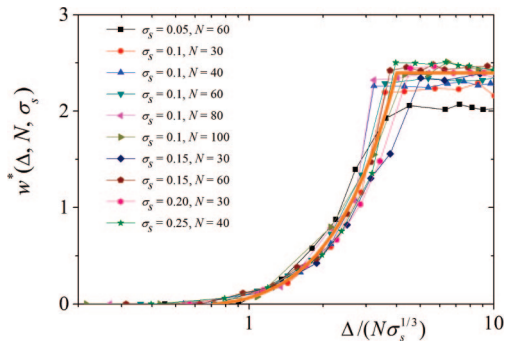


Figure 5. Plot of the calculated reduced average groove depth, $w_{0.05}^*(\Delta, N, \sigma_s) \equiv \bar{w}_{0.05}(\Delta, N, \sigma_s) / \bar{z}(\Delta, N, \sigma_s)$, as a function of $\xi = \Delta/(N\sigma_s^{1/3})$, together with the plot (solid line) of eq 3.

In Figure 4a–c we show representative density profile plots for the system with $N = 40$, $\sigma_s = 0.1$ and for various stripe widths, Δ . In these plots, the $\phi_0 = 0.05$ and $\phi_0 = 0.08$ perimeters of the brush are highlighted with yellow and red colors, respectively. Clearly, for $\Delta = 80$ ($\xi > 2.5$) the system appears as a sequence of independent sub-brushes above the grafting stripes (Figure 4c). On the other hand, for $\Delta = 20$ and $\Delta = 40$ ($\xi < 2.5$) (Figure 4a,b, respectively), the lateral extension of the sub-brushes becomes greater than half of the stripe width, and the polymers form a continuous layer that fully covers the

patterned substrate. However, in this region, and for small values of Δ (or, in the general case, for small values of ξ), the outer surface of the polymer layer appears statistically flat, resembling the morphology of a homogeneously grafted brush. On the other hand, for intermediate values of Δ , the outer surface of the film exhibits a wavy structure, as clearly depicted in Figure 4b. The periodicity of this pattern along the x -axis is the same with the periodicity of the substrate, and its maxima and minima are located on average above the midpoints of the grafted and the empty stripes, respectively. Interestingly, for these values of Δ , the polymer layer exhibits well-defined pores in the form of parallel tunnels above the nongrafted stripes. These three distinct polymer film morphologies are observed in all the studied systems upon changing the width of the grafting stripes.

To quantify our previous analysis of the morphology of the patterned brush and, more importantly, to determine the boundaries between the identified regimes as a function of Δ , N , and σ_s , we have calculated the average groove depth $\bar{w}_{\phi_0}(\Delta, N, \sigma_s)$ for all the systems studied. We define this quantity as the difference between the average height, h_{ϕ_0} , of the polymer film at the crests and the corresponding height at the troughs of the wavy pattern. The subscript ϕ_0 is used to indicate the local monomer density used for the determination of the perimeter of the brush. Clearly, for a patterned brush with a flat outer surface, $\bar{w}_{\phi_0}(\Delta, N, \sigma_s)$ goes to zero. It takes its maximum value when the system is in the nonoverlapping sub-brush regime. The results are presented in Figure 5 where we plot, as a function of ξ , the reduced groove depth, $w_{\phi_0}^*(\Delta, N, \sigma_s) = \bar{w}_{\phi_0}(\Delta, N, \sigma_s) / \bar{z}(\Delta, N, \sigma_s)$ calculated at the $\phi_0 = 0.05$ density level, i.e., the average groove depth $\bar{w}_{0.05}(\Delta, N, \sigma_s)$ scaled with the overall average brush height $\bar{z}(\Delta, N, \sigma_s)$. Again, all the data points collapse with good accuracy to a single curve. This suggests that the average groove depth is a universal function of ξ . From this plot it becomes clear that, when $\xi < \xi_1 \approx 0.7$, the brush exhibits a structureless, statistically flat, outer surface. At the other extreme, when $\xi > \xi_2 \approx 4$, all the systems are in the uncorrelated sub-brush regime. In the intermediate regime, $\xi_1 < \xi < \xi_2$, the outer surface of the brush exhibits the characteristic grooved morphology and parallel pores above the nongrafting stripes. In this regime both the depth of the grooves and the dimensions of the pores above the nongrafting stripes increase monotonously with ξ . It should be noted here that the values of ξ_1 and ξ_2 depend on the choice of the local monomer density, ϕ_0 , used to define the perimeter of the brush. However, our results indicate that for any $\phi_0 < 0.1$, $\bar{w}_{\phi_0}(N, \Delta, \sigma_s)$ is a universal function of ξ . Working with $\phi_0 = 0.05$, the calculated data of $w_{0.05}^*(\xi)$ are described satisfactorily by a functional dependence of the form

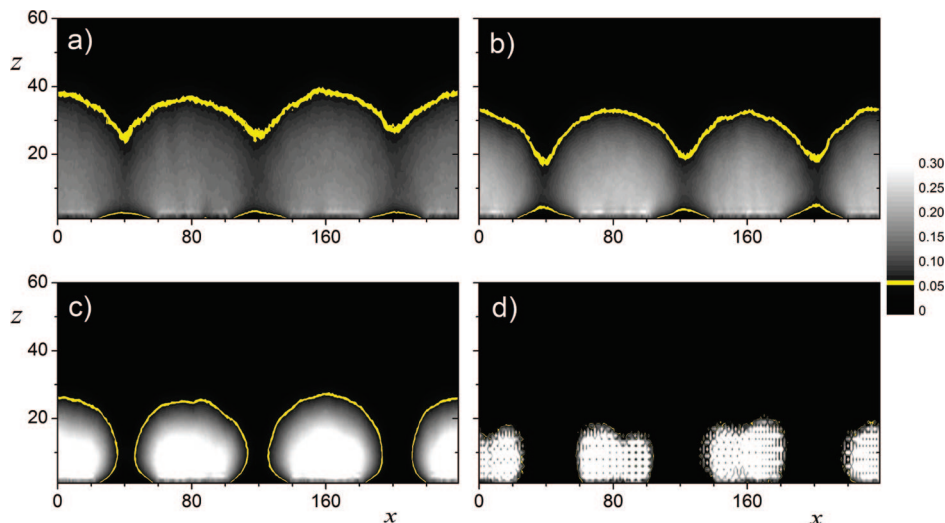


Figure 6. Calculated contour plots of the average two-dimensional density profile $\varphi(x,z)$ for a system with $N = 40$, $\sigma = 0.1$, and $\Delta = 40$ ($\xi = 2.15$) for various solvent qualities. The $\phi_{0.05}$ perimeter of the brush is highlighted. (a) $\varepsilon/k_B T = 0$, very good solvent; (b) $\varepsilon/k_B T = -0.3$, good solvent, the system is above the Θ -point; (c) $\varepsilon/k_B T = -0.5$, the system is close to its Θ -point;³⁷ and (d) $\varepsilon/k_B T = -0.7$, bad solvent. Note here that the unit length of the y -axis is twice that of the x -axis.

$$w_{0.05}^*(\xi) = \begin{cases} 0 & , \quad \xi < \xi_1 \\ a(\xi - \xi_1)^b & , \quad \xi_1 < \xi < \xi_2 \\ a(\xi_2 - \xi_1)^b & , \quad \xi > \xi_2 \end{cases} \quad (3)$$

The solid line in Figure 5 is the plot of Eq. (3), with parameters $a = 0.4$, $b = 3/2$, $\xi_1 = 0.7$ and $\xi_2 = 4$. On the other hand, for $\phi_0 > 0.1$ our results indicate that the corresponding perimeter of the brush is strongly affected by the periodicity of the patterned substrate and $w_{\phi_0}^*(\xi)$ reflects primarily the periodicity of the substrate instead of the true morphology of the outer surface of the brush. Practically speaking, the measurement of the outer surface inhomogeneities of such systems in the low ξ regime by scanning probe microscopy is restricted by the requirement that the scanning probe should be sensitive in the measurement of forces stemming from the $\phi_0 > 0.1$ density levels. This limitation was already pointed out by Patra and Linse in connection with their related atomic force microscopy studies in nanopatterned brushes.^{17,18}

Working in the $\xi_1 < \xi < \xi_0$ regime and combining the power law of eq 3 and eqs 1 and 2, the average groove depth can be written as $\bar{w} = \bar{z}_u(N\sigma_s/2) \times a(\xi - \xi_1)$. Taking into account that, for good solvents, \bar{z}_u in the semidilute regime scales as $N\sigma_s^{1/3}$, we obtain $\bar{w} \propto \Delta(\xi - \xi_1)^b/\xi$. A consequence of this proportionality is that, at constant ξ , the depth of the grooves increases linearly with the width of the stripes, Δ , provided that $\xi < \xi_0 = 2.5$. This means that we can obtain a specified groove depth for various stripe widths by tuning properly N and/or σ_s , provided that we keep ξ constant.

So far we studied exclusively systems under good solvent conditions. Simulations performed for poorer solvents ($\varepsilon/k_B T < 0$) indicate that the quality of the solvent strongly affects the morphology of the polymer brush. We have studied in detail the solvent (temperature) effects for the system with $N = 40$, $\sigma_s = 0.1$, and $\Delta = 40$ (yielding $\xi = 2.15$). Calculated two-dimensional density profiles at various solvent conditions are presented in Figure 6a–d. Taking into account that the Θ -point, as calculated in ref 38 with the same parametrization adopted in our study, is $(\varepsilon/k_B T)_\Theta \approx -0.52$, the presented density profiles correspond to systems (i) under good solvent conditions (Figure 6a,b), (ii) close to the Θ -point (Figure 6c), and (iii) under

a very poor solvent (Figure 6d). Clearly, as the quality of the solvent worsens, chains tend to congest above the occupied stripes, and both the depth of the grooves and the size of the pore above the nongrafting stripes increase. Below the Θ -point, the brushes on each stripe fully separate and form dense column-like structures where the lateral expansion of the sub-brushes is very limited (see Figure 6d). However, the “crystallization” within the columns at these very low temperatures is mainly due to the lattice nature of the bond fluctuation model, and this effect should not be expected in real grafted chains.^{37,38} These results demonstrate clearly that it is possible to tune, in a controllable fashion, the morphology of the outer surface of the nanopatterned brush by changing the solvent conditions.

Conclusions

In conclusion, our results suggest that, under good solvent conditions, the average brush height, when scaled with the mean height of the equivalent homogeneously grafted brush, is a universal function of the combined parameter, $\xi = \Delta/N\sigma_s^{1/3}$. For $\xi < \xi_0 \approx 2.5$, the average height of the patterned brush coincides with the height of a nonpatterned brush with surface coverage $\sigma = \sigma_s/2$. On the other hand, for $\xi > \xi_0$, eq 3 satisfactorily describes the ξ -dependence of the scaled average height. Therefore, ξ_0 constitutes a critical parameter that defines the combinations of N , σ , and Δ for which the average height of the patterned brush starts to deviate from the corresponding height of a homogeneous brush having the same overall grafting density.

Furthermore, we have identified in terms of ξ three different regimes with distinct brush morphology. For $\xi < \xi_1 \approx 0.7$, the polymer film has properties similar to those of a homogeneously grafted brush with grafting density $\sigma_s/2$. For $\xi > \xi_2 \approx 4$, the tethered polymers form a sequence of isolated sub-brushes extended above the grafting stripes. More interestingly, for $\xi_1 < \xi < \xi_2$, the polymer layer exhibits parallel pores above the nongrafting stripes and a grooved outer surface. The relative depth of the grooves is a universal function of ξ .

The proposed analysis of the structural properties of the specific nanopatterned brushes studied here, in terms of a single parameter

$\xi = \Delta/N\sigma_s^{1/3}$ provides clear guidelines for designing and fabricating well-defined and controllable polymeric films. These systems may serve as soft templates for the manipulation and possibly for the ordering of nanoparticles of various sizes. Furthermore, the predetermined directionality of the stripes together with the tunable depth of the grooves could be utilized to provide thermodynamic and mechanical control on liquid crystalline order. Finally, an interesting feature of these systems

is that they offer the possibility for a precise control of their pattern by changing the solvent quality.

Acknowledgment. We would like to thank Dr. Costas Daoulas for useful discussions on the results of this work. Support by the Hellenic GSRT through the programme PENED03 (project NYVRIFOS) is also acknowledged.

LA802536V